eXPRESS Polymer Letters Vol.14, No.7 (2020) 638–650
Available online at www.expresspolymlett.com
https://doi.org/10.3144/expresspolymlett.2020.52

Cellulose nanocrystal reinforced acylglycerol-based polyurethane foams

M. V. Gangoiti[1], *P. J. Peruzzo*[2,3*]

[1]Laboratorio de Investigaciones en Osteopatías y Metabolismo Mineral – LIOMM (CIC-PBA), Facultad de Ciencias Exactas – UNLP, 47 y 115, (B1900AJL) La Plata, Argentina
[2]Instituto de Investigaciones Fisicoquímicas Teóricas y Aplicadas – INIFTA (UNLP – CONICET CCT La Plata), Diag. 113 y 64, (B1904DPI) La Plata, Argentina. CC 16 Suc. 4
[3]Universidad Nacional Arturo Jauretche – UNAJ, Av. Calchaquí 6200, (1888) Florencio Varela, Argentina

Received 4 September 2019; accepted in revised form 25 November 2019

Abstract. This work presents the preparation of polyurethane composite foams based on castor oil or modified canola oil as a polyol, and cellulose nanocrystals (CN) as nanofiller (0.10, 0.25, and 0.50 wt% of CN content). The bio-based composites were characterized by Fourier Transform Infrared Spectroscopy (FTIR), Scanning Electron Microscopy (SEM), Differential Scanning Calorimetry (DSC), Thermogravimetric Analysis (TGA), and mechanical properties. The SEM images showed that composite foams had smaller cell sizes and more irregular than those observed for unloaded samples. FTIR revealed that the urethane/urea bond formation was influenced by the incorporation of CN, and was dependent on the polyol used in the formulation. The incorporation of CN did not affect the thermal stability, but the density and mechanical properties changed differently depending on the selected polyol. These results suggested that the acylglycerol structure affects the role of CN in the formulation. Also, the proliferation of MC3T3-E1 preosteoblastic cells showed that the cell viability of polyurethane bionanocomposite foams increased significantly in comparison to the unloaded material.

Keywords: *biocomposites, polyurethane biofoams, acylglycerol polyols, cellulose nanocrystal, cell viability*

1. Introduction

Renewable resource-derived polymers and their composites have attracted attention in recent years due to increasing environmental concern and restricted availability of petrochemical resources. In this way, polyurethanes (PU) obtained by the incorporation of a bio-based substitute of the petrochemical raw materials have become an issue of interest [1]. PU are systems composed of soft (SS) and hard segments (HS), which are obtained from the polyol and isocyanate precursors, respectively. The chemical industry of PU has recently paid intense interest to the production of bio-based polyols, mainly those synthesized from vegetable oils [2], instead of the use of isocyanate precursors from renewable resources. This is because isocyanates still depend on petroleum feedstocks, and research has not led to an industrially viable synthesis path [1]. Typically, castor oil and its derivatives are selected as polyols [3], but other oils like soybean oil and rapeseed oil have been used to a lesser extent after chemical modification to incorporate reactive hydroxyl groups in the structure [4, 5].

Within the wide variety of ways and forms in which PUs can be obtained, polyurethane foams (PUF) represent a relevant class of PU materials with several applications, ranging from insulation panels, structural reinforcement, and sandwich construction, among others like biomedical or electrical applications [6]. Bio-based PUF obtained from vegetable

*Corresponding author, e-mail: pjperuzzo@inifta.unlp.edu.ar

oil-based polyols have also been extensively studied, in particular from castor oil-based polyols. The works in this area reported that increases in the biopolyol content improve some properties of the final product like hydrophobicity (higher water contact angle, lower water uptake), and tensile modulus [7]. In PUF synthesized totally from vegetable oil-based polyols, the functionality and reactive group position affect the PU network, changing, in consequence, the cell structure and the mechanical and thermal properties of the final product [8, 9]. Due to the hydrophobic nature of the vegetable oil-based polyols, they produced PUF with enhanced thermal stability, hydrophobicity, and hydrolytic stability. Although similar results were obtained for PUFs based on other vegetable oil-based polyols, they have not been extensively studied [10–12]. Despite the improvement of some properties of the biobased PUF as we described above, they are generally inferior when are compared to the properties of the petroleum-derived counterparts [13]. For this reason, it is common to prepare composites to cope with limitations such as low stiffness and low strength of PUF derived from vegetable oils [14, 15]. The introduction of nanomaterials into polymeric composite foams has garnered much attention because nanofillers are proven able to affect the foam morphology, and can also change the mechanical/rheological properties of the polymer matrix. Further, they could add additional functionality, such as electrical conductivity, thermal stability, and gas permeability [16]. Nanofillers such as glass fiber [14] clay [17, 18], silica [19], carbon fiber [20] and carbon nanotubes [21] have been used to enhance the mechanical properties and to confer new properties to the bio-based PUF composites. But the addition of nanofillers to PUF is also known to have variable effects depending on the percentage of loading and the size of particles [6,16], even more, if the filler changes the NCO/OH ratio interfering on the rate of the foaming process. If the improvement of the properties is achieved by the incorporation of a filler, PUF composites can reduce the weight, energy, and cost of the material/application. Also, this strategy allows reducing the weight fraction of the hard segment and increasing as a consequence, the content of renewable component in the formulations. This is more favored if the nanoparticles are obtained from renewable resources. Thus, cellulose nanocrystals (CN) have gained particular attention in recent years, not only for its unique physical and chemical properties but also for its inherent capacity for renewal and sustainability, in addition to its abundance [22].

The incorporation of CN to different polymer matrices has been extensively studied in the last years [23], and PUF was no exception [24, 25]. However, few studies of PUF obtained totally from vegetable oil-based polyols, and reinforced with CN have been published so far [26–30]. These works showed that CN incorporation affected the cell size, mechanical properties, dimensional stability, and water uptake of the foams. On the other hand, the addition of CNs decreased the thermal stability of PUF [28, 29]. Because these works are based on different raw materials, it is difficult to obtain a general structure-property relationship of these foams. But they demonstrated that CN acted as reactive reinforcing filler, as well as nucleation agent and/or particulate surfactant depending on the Isocyanate index and the NCO number of the isocyanate [27, 28], affecting as a consequence the properties. In this way, the effect of changing the polyol on the role of CN in the formulation has not been taken into account. For polyols chemically similar, structural differences between them could affect the role of CN in the formulation. As a consequence, properties of the PUF could vary differently with the CN incorporation depending on the selected polyol. Therefore, the present work deals with the preparation of biocomposite PUF based on castor oil (CO) or modified canola oil (CanP) as polyol, and cellulose nanocrystals (CN) as nanofiller. They were characterized by FTIR, SEM, TGA and mechanical properties. Because many works claim that these materials have potential applications in the field of biomedical engineering, cell viability was also evaluated.

2. Experimental section

2.1. Materials

Castor Oil (CO, Anedra 99.9%, Argentina) was used as polyol, with N° OH = 164.3 mg KOH/g and acidity value of 0.8 mg KOH/g (approx. functionality 2.7) determined according to ASTM D4274-99 (Test Method A). Canola Oil (CanO, Amerika 2001, Argentina), Formic Acid 85% (Anedra, Argentina), H_2O_2 30% (Biopack, Argentina); HBF_4 (Merck, Germany); MeOH (Cicarelli, Argentina), Dibutyltindilaurate (DBTDL, 95%, Sigma-Aldrich, U.S.A.) were used as received. Poly(methylene diphenyldiisocyanate) (pMDI, Suprasec 9634, Huntsman, U.S.A.), with a functionality of 2.15 and an NCO number of

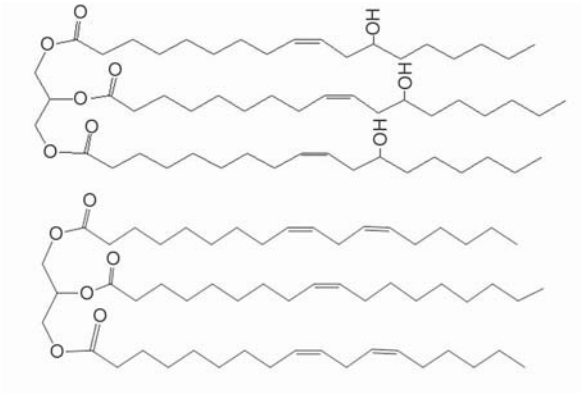

Figure 1. Idealized chemical structures of castor oil (above) and canola oil (down).

29.5 (determined according to ASTM D2572-97) was provided by Química R&F S.R.L. (C.A.B.A., Argentina), and silicone-based surfactant (TEGOSTAB8409, Evonik, Germany) and the catalyst (TEGOAMIN41, Evonik, Germany) were kindly provided by Mayerhofer Argentina S.A. (C.A.B.A., Argentina). Distilled water was used as the blowing agent. The commercial CN was provided by the University of Mayne, which are rod-shaped particles of about 7 nm in diameter and 160 nm in length [31, 32]. Chemical structures of vegetable oils are presented in Figure 1.

2.2. Preparation of canola based polyol

Canola oil (CanO) was epoxidized using performic acid generated *in situ*, adapted from different techniques [5, 33]. Formic acid (16.40 ml) was added on canola oil (107.33 g), and the mixture was cooled in an ice-water bath. Then, hydrogen peroxide (110.00 ml) was added drop by drop, and the reaction mixture was placed at 30 °C for 24 h under mechanical stirrer. Later, the organic phase was washed twice with water, $NaHCO_3$ saturated solution (2×30 ml), and water until neutral pH. After drying, different from the other techniques, the epoxidized canola oil (ECO) was crystallized from solution at low temperature. Thus, materials present in the natural oil which did not react o were chemically different from the product remained in solution. The solid was filtered and dried until constant weight (61.88 g). To obtain a polyol by the ring-opening reaction of the epoxide group, the dried ECO (60.00 g) was added to a solution of MeOH (80.00 ml) and HBF_4 (1.20 ml). The reaction mixture was mechanically stirred at 60 °C for 3 h. Finally, 100 ml of ethyl acetate was added, and the organic layer was washed with water, then with $NaHCO_3$ and brine, dried with

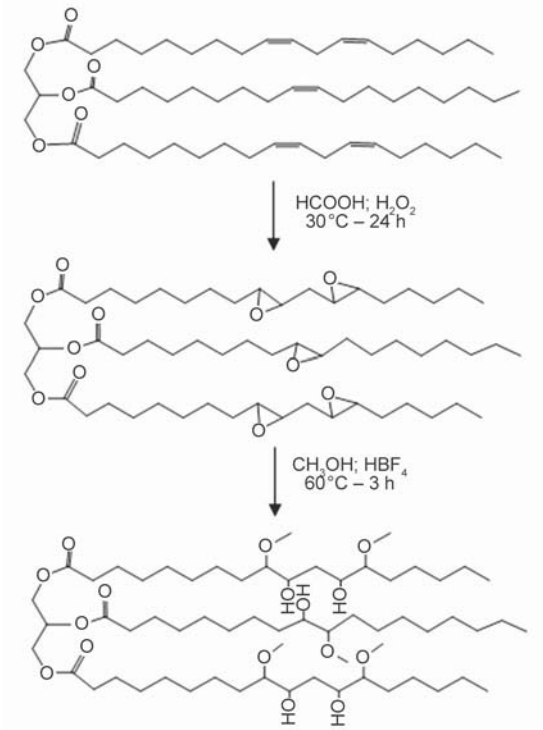

Figure 2. Scheme of synthesis of canola polyol (CanP).

anhydrous Na_2SO_4, filtered, and finally concentrated using a rotary evaporator. This produced a light yellow transparent oily product, coded as Canola polyol 'CanP' (57.60 g), with a hydroxyl value of 183.8 mg KOH/g (approx. functionality 3.3) and acidity value of 0.2 mg KOH/g determined by ASTM D4274-99 (Test Method A). The scheme of reaction and FTIR characterization of products are shown in Figures 2 and 3, respectively. In the canola oil spectrum, it was possible to observe the signals at 3006 cm^{-1} ($\nu_{=C-H}$) and 1652 cm^{-1} ($\nu_{C=C}$) related to the presence of double bonds in the canola oil. After epoxidation, the spectrum of the product (epoxidized canola oil) showed the peak related to the presence of the epoxy

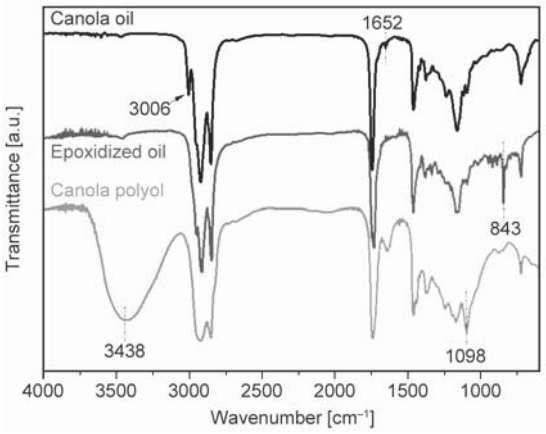

Figure 3. FTIR spectra of canola oil, epoxidized canola oil and canola polyol (CanP).

groups at 843 cm^{-1} without evidence of $\nu_{=C-H}$ and $\nu_{C=C}$ signals. After polyol formation by reaction with methanol, new bands at 3438 cm^{-1} (ν_{O-H}) and 1098 cm^{-1} (ν_{C-O-C}) were observed, while any band related to the epoxy ring was observed [34, 35].

2.3. Foams preparation

The foams were prepared by free-rising in a mold at room temperature [29]. First, the polyol, catalysts, surfactant and blowing agent were mixed for 30 s under mechanical stirring in a plastic beaker. After that, CN was added and mixed for 2 min. When the mixture became homogeneous, pMDI was added and vigorously stirred for 20 s, and then the foaming began after a short time. Finally, white, semi-rigid foam was obtained within a few seconds. Neat polyurethane foams were prepared using a similar foaming process in the absence of CN. The foam was removed from the foaming beaker after 1 h and allowed to post-cure at room temperature for 1 week before the characterization. The formulations used are shown in Table 1, where the parts of each component are based on per hundred parts of the polyol, designated as php. A shorthand notation was used in this work where, for instance, CanP-0.25 represents a nanocomposite polyurethane foam based on canola polyol containing 0.25 wt% of CN.

2.4. Characterization

Apparent density was calculated as the ratio between the weight and the volume of a cubic specimen (25 mm side). At least five replicated specimens of each sample were measured.

FTIR spectra of samples were obtained using a IRAffinity-1 spectrophotometer (SHIMADZU CORPORATION, Japan) in DRIFT mode (64 scans for experiment and a resolution of 4 cm^{-1}). For comparison, the characteristic absorbances were normalized using the C–H absorbance at 2935 cm^{-1} as the standard.

The morphology of the cross-section of the foams was observed by Scanning Electron Microscopy (SEM) using a Jeol JSM-6460 microscope (JEOL Ltd, Japan). The samples were sputtered with a Au-Pd mixture before observation.

Thermogravimetric analysis (TGA) was obtained using a TA Q2000 instrument (TA, U.S.A.) running about 5 mg sample from room temperature to 60 °C at a heating rate of 10 °C·min^{-1} in N_2 atmosphere.

The compression properties of the films were measured at 25 °C using a DIGIMESS TC-500 tensile-testing machine (DIGIMESS, Argentina). Specimens of 4 cm width and 4 cm length and 1 cm tall were prepared, and a testing speed of 5 mm·min^{-1} was used until 40% of deformation. The results were the average of five valid measurements.

For cytotoxicity assays, MC3T3-E1, a line of preosteoblastic cells, were used. Cells were maintained in basal media (DMEM-10% FBS) at 37 °C. Cell proliferation was evaluated by the 3-(4,5-dimethylthiazol-2-yl)-2,5-diphenyl tetrazolium bromide (MTT) assay. MTT is converted to water-insoluble, dark blue MTT-formazan by mitochondrial dehydrogenases of living cells. Thus, absorbance change is directly proportional to the number of viable cells. Briefly, $2.5 \cdot 10^4$ cells per well in basal media were plated onto the scaffolds, which were cast on multiwell culture plates and cultured for 24 hours. After these culture periods, cells were incubated for two additional hours with a solution of 0.1 mg·ml^{-1} MTT. Passed this time, stained cells were observed using a Nikon Eclipse TS100 inverted optical microscope (Nikon, Japan) and photographed. Then, after washing, the formazan precipitate was dissolved in dimethyl sulfoxide (DMSO), and the absorbance read at 570 nm.

Table 1. The recipe used in this work.

Component	Role	Castor oil [php]	Canola polyol [php]
Part A			
CO or CanP	polyol	100	100
TEGOSTAB8409	surfactant	2	2
TEGOAMIN41	catalyst	0.5	0.5
DBTDL	catalyst	0.5	0.5
WATER	blowing agent	3	3
CN	reinforcement	0; 0.2; 0.5; 1	0; 0.2; 0.5; 1
Part B			
pMDI	isocyanate	93.6	98.8

A/B index: ~1.1
Isocinate Index: 105

3. Results and discussion

3.1. Foaming process

Both polyols used in this works are acylglycerols with secondary –OH groups and similar dangling chain length, but they are different in functionality and the access to the –OH group. In CanP there are neighboring CH_3O– groups that cause steric hindrance to the –OH reactive group; instead a cis double bond is present near to the –OH group in the fatty

Table 2. Foam behavior parameters (t_c: cream time; t_r: end of rise time; t_t: tack-free time) of foams obtained in this work.

CN content	Castor oil			Canola polyol		
	t_c [s]	t_r [s]	t_t [s]	t_c [s]	t_r [s]	t_t [s]
0	10±2	42±4	50±4	34±2	90±5	170±8
0.1	9±3	40±3	50±3	30±2	103±3	180±9
0.25	9±2	41±3	51±3	34±2	108±4	185±6
0.5	8±2	40±3	50±5	32±3	102±5	180±8

acid chains of CO. Table 2 shows the foaming behavior of the samples obtained in this work. The cream time (t_c), end of rise time (t_r) and tack-free time (t_t) were higher for CanP-based PUF comparing to CO-based samples. This can be attributed to the more sterically hindered –OH groups in the CanP polyol due to the neighboring –OCH_3 groups, which affect the reactivity and consequently the rate of expansion and gelation time [29, 36]. For each series (CO or CanP), tc, tr and tt were similar for composite samples with different CN content. However, tr and tt slightly increased for the composite samples based on CanP polyol respect to the CanP-0 sample. This indicated that the incorporation of the CN did not affect significantly foaming behavior when CO is used in the formulation [29], but had an impact in the case of CanP.

3.2. FTIR results

Figure 4a shows the FTIR spectra of CN and PUF without and with 0.5 wt% of CN. The PU spectrum showed the typical band at around 3335 cm^{-1} arising from ν_{N-H} mode (free and H-bonded), an absorption at 1720 cm^{-1} related to the PU Amide I band ($\nu_{C=O}$ in urethane bond) overlapped to $\nu_{C=O}$ of –COO– groups present in natural polyols, and a band centered at 1557 cm^{-1} (Amide II band, $\delta_{N-H} + \nu_{C-N} + \nu_{C-C}$). For the pure CN the band between 3600 and 3200 cm^{-1} was related to the O–H stretching vibrations, and the absorption bands between 300–2800 and 1500–1250 cm^{-1} regions came from the C–H and C–H_2 stretching and bending vibrations, respectively. Besides, it was also possible to observe the band related to the glycosidic linkage (1155 cm^{-1}) and the strongest band located between 1100–970 cm^{-1} dominated by ring vibrations overlapped with stretching vibrations of C–OH side groups, and at 1029 cm^{-1} the C–O–C stretching in the pyranoid ring [37, 38]. Incorporating CN did not introduce changes in the intensity of the regions

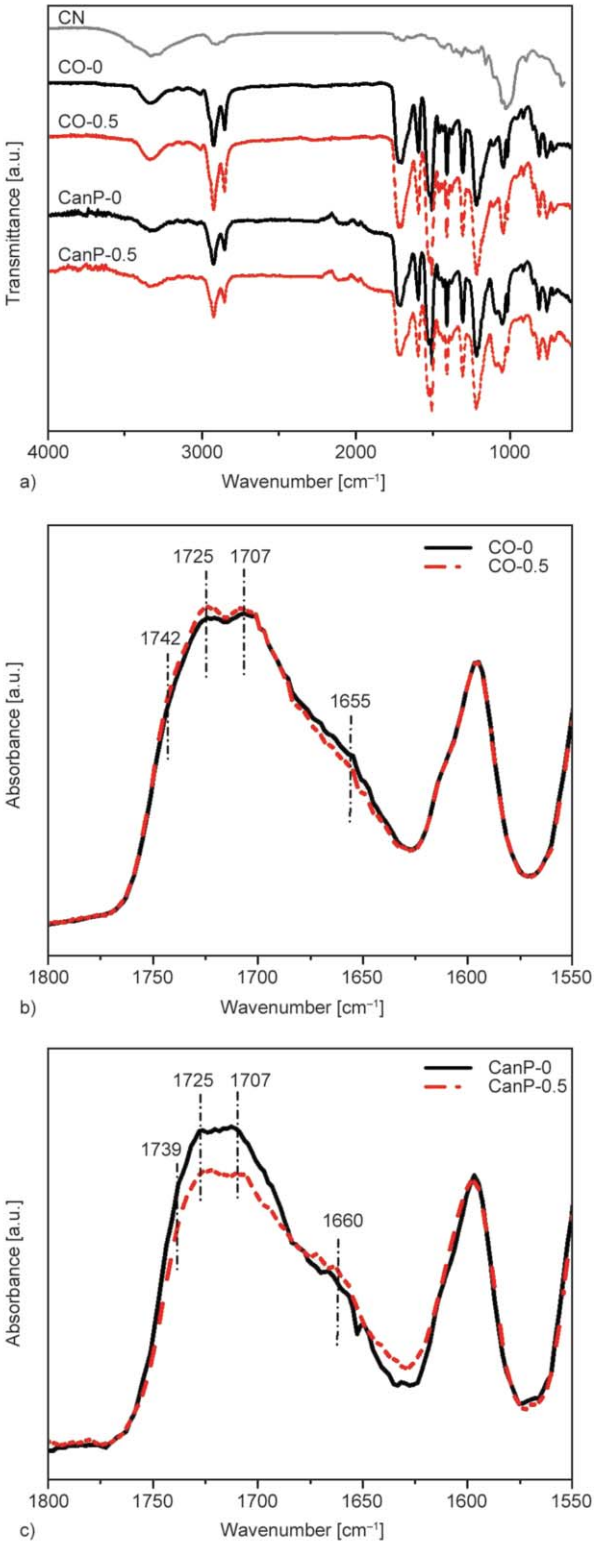

Figure 4. a) FTIR spectra of CN, PUF, and nanocomposites PUF containing 0.5 wt% of CN. b) Carbonyl region for samples CO-0 and CO-0.5; c) Carbonyl region for samples CanP-0 and CanP-0.5.

around 1100 or 3300 cm^{-1} (C–O–C and O–H in CN, respectively) due to the lower CN content of the samples of this work [27]. Instead, changes were

observed in the C=O region. When this region was observed in detail (Figure 4b and 4c), it was possible to detect the contribution of the carbonyl stretching vibration of C=O groups belonging to the ester groups present in the triglycerides at around 1740 cm^{-1} [39], the signals at 1725 cm^{-1} and 1701 cm^{-1} related to free and H-bonded $\nu_{C=O}$ of the urethane linkage, respectively, and the band located at 1650 cm^{-1} assigned to the $\nu_{C=O}$ in urea bonds. In the case of CO-based samples, a slight decrease in the formation of urea bonds and the formation of additional urethane linkages were observed with the incorporation of CN (Figure 4b), suggesting that –NCO groups reacted with the hydroxyl groups at the CN surface changing the internal organization of the PU matrix. Instead, a noticeable decrease in the relative amount of urethane groups in the CanP based foams containing CN was detected, indicating that CN interacts with the SS when this polyol is used in the formulation. This would lead to a reduction in the availability of –OH groups of both materials preventing the formation of urethane groups. These results are in agreement with that observed by other authors [28], suggesting in this case that incorporating CN modified the urethane and urea kinetics. However, they changed in a different way depending on the polyol used in the formulation, in accordance with the foaming behavior previously presented.

3.3. SEM results

Optical and SEM images of the prepared foams are shown in Figure 5. PUF and composites obtained from CO are light-yellow comparing to those obtained from CanP, which were whiter foam and with larger cell size. Besides, CO-based samples were closed cell foams, whereas open-cell foams were obtained from CanP. Incorporating CN resulted in foams with smaller cell sizes and anisotropic, having a larger dimension parallel to the growth direction (Figure 5c and 5d). Table 3 shows the cell dimensions on the direction parallel (L) and perpendicular (T) to the growth direction, and the anisotropic factor ($r = L/T$), which resulted similar for all the nanocomposite foams independently of both the polyol and CN content. The fact that CanP-0.1 presented cell dimensions between CanP-0 and CanP-0.25 suggested that polyol characteristics seem to have an effect on the cell dimensions of the nanocomposite foams at lower CN content. However, cell size was similar when CN content higher than 0.25 wt% was used, regardless of the selected polyol. Thus, the addition of CN decreased the cell dimensions for both series (CO and CanP) suggesting that CN provides sites which facilitate the nucleation process [27], with opposite effect on the density of the foams (as can be observed in the next section) depending on the polyol used in the formulation.

3.4. Properties of foams

Reference PUF samples (CO-0 and CanP-0) presented density values of 51 and 59 $kg \cdot m^{-3}$, respectively, where the difference can be explained based on the polyol properties (OH– functionality). When density values of the nanocomposite foams were observed, samples obtained from CO showed higher density comparing to the reference sample CO-0, while composite samples based on CanP presented a lower density than the unloaded material. The results are in agreement with the FTIR observations, where the decrease in the formation of urea bonds in the CO-based composite foams could be associated with a lower blowing gas production, and consequently, higher density was obtained for these samples. In the case of CanP-based composite foams, a lower urethane bond production avoids the formation of the polymer matrix and consequently the density decreases. Thus, the addition of CN changed the growth stage in a different way depending on the polyol used, but independently of the CN content for the formulation used in this work.

The results of the compression tests, compressive elastic modulus (E), and strength (σ) are presented in Table 4. In general, the incorporation of the nanofiller improved the mechanical properties of PUFs. In both series (CO and CanP based samples) an increase of the compressive modulus E was observed for all the samples regardless of CN content. However, the compressive strength σ of the PUFs based on CO increased as CN content increases, while the biobased foams based on CanP maintained a similar value of σ regardless of the CN content. These observations were maintained indeed when density was taken into account to obtain the specific strength (σ/d) and specific modulus (E/d) (Table 4). The specific strength of CanP based composites increases by about 10%, independently of the CN content. Instead, in CO-based composites, the specific strength increases gradually up to 300% for CO-0.5 sample, in agreement with the participation of CN as HS in the formation of the polymeric matrix. Indeed, while

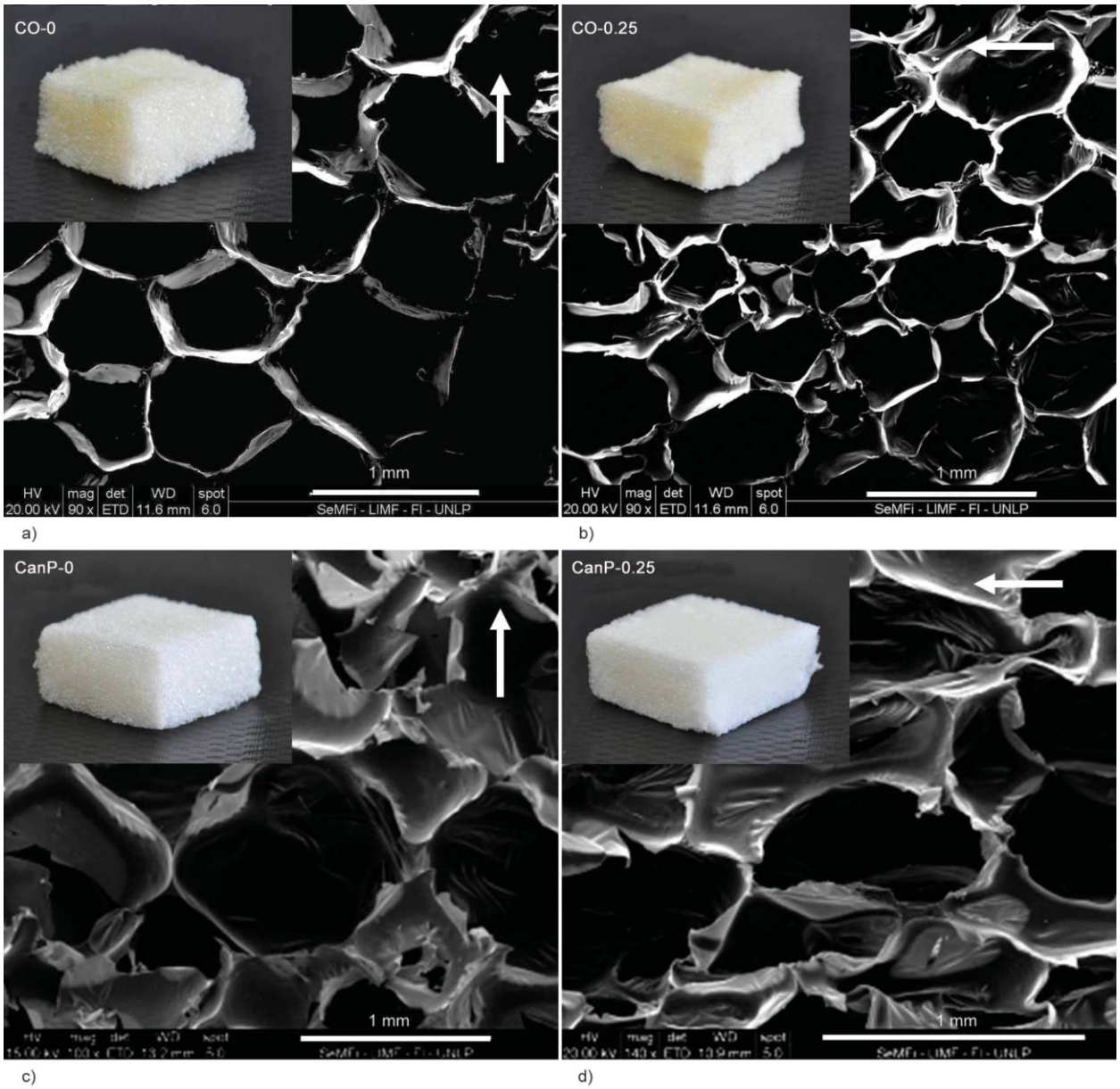

Figure 5. Optical and SEM images of polyurethane foams and nanocomposite PUF with 0.25 wt.% CN content. Arrows indicate the PUF growth direction. a) CO-0 sample; b) CO-0.25 sample; c) CanP-0 sample; and d) CanP-0.25 sample.

Table 3. Cell dimensions of PUFs obtained in this work.

	Castor oil				**Canola polyol**			
	CN content [wt%]				**CN content [wt%]**			
	0	**0.1**	**0.25**	**0.5**	**0**	**0.1**	**0.25**	**0.5**
L [mm]	0.70±0.16	0.71±0.11	0.70±0.14	0.68±0.17	0.92±0.14	1.09±0.20	0.76±0.18	0.79±0.15
T [mm]	0.78±0.16	0.43±0.08	0.37±0.07	0.43±0.10	0.87±0.15	0.63±0.18	0.45±0.14	0.46±0.10
$r = L/T$	0.90	1.66	1.89	1.58	1.06	1.73	1.70	1.72

L: cell dimension in the growth direction, *T*: cell dimension in the perpendicular growth direction

specific modulus increase as CN content increase for CO based samples, higher amounts CN seems to be detrimental to this parameter in the CanP series. This is probably due to the interaction of the filler with the SS and, as a consequence a lower urethane linkage formation in agreement with FTIR results.

Plots from TGA and dTGA of CN, PUFs, and nanocomposite foams containing 0.25 wt% of CN content

Table 4. Density and mechanical properties of the BPU foams.

Sample	d [kg/m^3]	$\sigma_{10\%}$ [kPa]	$\sigma_{10\%}/d$ [kN·m·K·g^{-1}]	E [kPa]	E/d [kN·m·K·g^{-1}]
CO-0	51±4	10±1	0.20	163±17	3.20
CO-0.1	63±1	22±5	0.35	503±132	7.99
CO-0.25	58±3	38±5	0.66	461±5	7.95
CO-0.5	61±2	51±11	0.84	705±57	11.56
CanP-0	59±4	38±5	0.64	182±11	3.09
CanP-0.1	48±5	35±4	0.73	563±128	11.74
CanP-0.25	51±3	33±6	0.65	624±142	12.23
CanP-0.5	50±3	36±6	0.72	408±102	8.17

are shown in Figures 6a and 6b, respectively. Also, the IDT (initial decomposition temperature) and the thermal indexes T_5 and T_{50} (temperatures corresponding to a 5% and 50% loss in weight) are shown in Table 5. TGA and dTGA curves of samples revealed noticeable differences in the whole temperature range depending on the polyol used in their synthesis. For CO-based samples, decomposition started at approximately 260 °C. On the other hand, samples based on CanP showed lower thermal stability, in which decomposition started at 220 °C, with lower T_5 and T_{50} than PUFs based on CO. Besides, dTGA curves revealed different behavior for the different decomposition steps, related to differences in the structures of the polyol. In general, thermal decomposition profile of bio-based PUF has been reported maximum in the dTGA curves at temperatures around 230–330 °C related to urethane bond decomposition [40], 350–390 °C attributed to ester/ether bond decomposition through chain scission [41, 42], and 430–470 °C (due to C–C bond cleavages [43]. In our case, dTGA curves of samples obtained from CO presented three decomposition steps, where the first peak at 309 °C in dTGA curve showed a shoulder at lower temperature. Instead, the first decomposition process of CanP samples presented two peaks located at 244 and 295 °C in the dTGA curve. This can be attributed to differences in the polymer network structures due to the different structure of the used polyols, where the secondary functional hydroxyl groups in the CanP are more sterically hindered and probably conduct to a low cross-linking density and less stable urethane bonds because they avoid the typical H-bonding organization of the PU [5, 8]. Furthermore, differences in the polyol structures also influenced the second thermal decomposition steps, probably due to differences in the dangling chain length, number of unsaturations, and the presence of ether bonds depending the polyol selected for the foam synthesis [4, 8, 44–46]. Incorporating CN produced a slight decrease in the thermal stability of both systems. This change seems to be related to a contribution of the decomposition of the CN around 300 °C (depolymerization, dehydration, and decomposition of glycosyl units) [47], and 440 °C (oxidation and decomposition of carbonaceous residue to gaseous products of low molecular weight) [48].

The results suggested that CN has a different role depending on the acylglycerol used in the formulation. Previous works have demonstrated that the CN in a

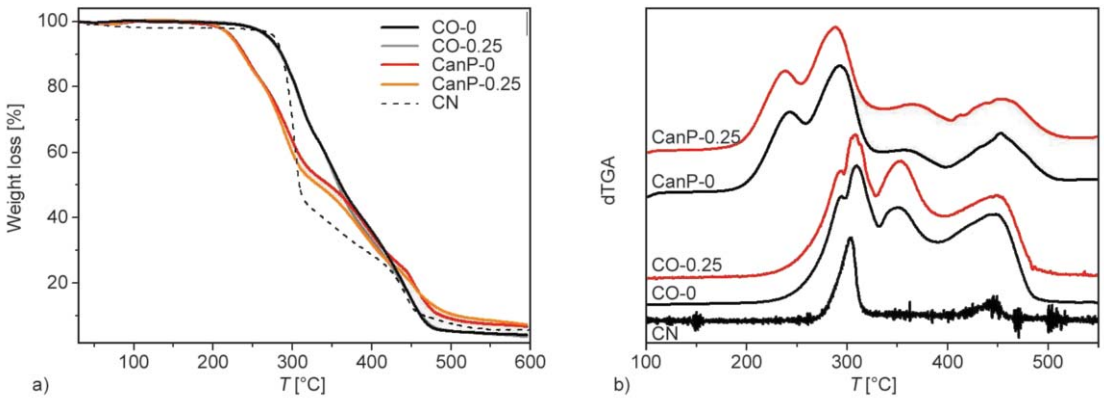

Figure 6. TGA (a) and dTGA (b) curves of selected samples obtained in this work.

Table 5. Thermal properties of the BPU foams.

Sample	TGA						
	IDT [°C]	T_5 [°C]	T_{50} [°C]	Td_1 [°C]	Td_2 [°C]	Td_3 [°C]	Td_4 [°C]
CO-0	265.40	271.43	360.94	294.98[a]	309.27	351.15	447.85
CO-0.1	260.53	265.03	354.01	292.90[a]	305.92	352.31	449.52
CO-0.25	265.58	269.83	356.68	292.85[a]	307.27	352.34	448.46
CO-0.5	259.62	259.17	351.88	293.86[a]	305.62	355.95	449.82
CanP-0	218.70	224.85	346.79	244.30	295.37	360.05	451.99
CanP-0.1	215.39	221.45	328.08	242.27	292.59	356.11	452.90
CanP-0.25	213.90	223.15	332.05	239.34	289.58	362.01	455.30
CanP-0.5	213.14	220.88	332.61	237.92	287.93	364.74	450.45

[a]shoulder at peak with maximum at Td_2

PUF can associate to the HS or SS in the polyurethane network and acting as nucleation agent or particulate surfactant, depending on the isocyanate index and NCO number of the isocyanate formulation as previously exposed [8, 27, 28]. In our case, the experimental results suggested that the acylglycerol-based polyol used in the formulation of the PUF also affects this behavior, where CN acted as a nucleation agent, with a migration to the HS in the case of the CO-based polyurethane foams, and to the SS in CanP based samples.

3.5. Cell viability

Many works related to bio-based PU or PUF claim that these materials have potential applications in the field of biomedical engineering. Even if the constituents are bio-based and well biocompatible, the resulting material is not necessarily biocompatible. So, it is necessary to conduct tests before indicating if a bio-based material can be considered as a potential biocomposite product [49]. The in-vitro biocompatibility of the biofoams obtained in this work was evaluated by MTT assay (Figure 7a) and the observation of the cell morphology (Figure 7b). Figure 7a shows that the incorporation of 0.1 wt% CN did not change the growth of cells. However, at concentrations of 0.25 and 0.5 wt% of CN both PUF-CO (Figure 7a/α) and PUF-CanP (Figure 7a/β) increased significantly the MC3T3-E1 cells proliferation with respect to the control (PUF without CN), being higher for samples based on CO. The evaluation of cell morphology after 24 h showed that cells survived and grew on the different materials, as it can be observed in Figure 7b for CanP-0 and CanP-0.25 samples as representative images. For samples without CN, it seems that the cells preferred to adhere to each other rather than grow on the surface and spread. However, for samples with 0.25 and 0.5 wt% of CN content, they were flattened on the surface with more spindle-like morphology, which was indicative that the cells proliferated and adhered strongly to the composite foams respect to the unloaded samples [50], these observations could be related to changes in the hydrophilicity of the materials due to the used polyol [51] and incorporation of CN [52]. Regardless of this, the obtained results were indicative of the improvement of the cell viability of the reinforced polyurethane foams at these CN concentrations.

4. Conclusions

This work presented the preparation of polyurethane biobased composite foams obtained from polymeric methylene diphenyl isocyanate, castor oil or modified canola oil as polyol, and different contents of cellulose nanocrystals. Polyurethane foams with a density of around 50–60 kg·m^{-3} were obtained. Incorporating CN they modified the morphology, leading to the production of foams with smaller cell sizes and more irregular than those observed for the matrix. Besides, improving the mechanical properties of the PU, biobased foams, without significant changes in thermal properties, were obtained. Taken as a whole, the variation of the properties with the incorporation of CN suggested that the chemical structure of the polyol affects the role played by CN in the formulation of the bio-based PUF. When CanP was used, the CN interacted better with the soft segment, which affected the urethane bond formation and resulted in a decrease in the foams´ density, and a slight improvement in mechanical properties. This was different in the case of CO, where CN took part in the urethane bond formation acting as a hard segment, with an increase of the composite foams´ density and

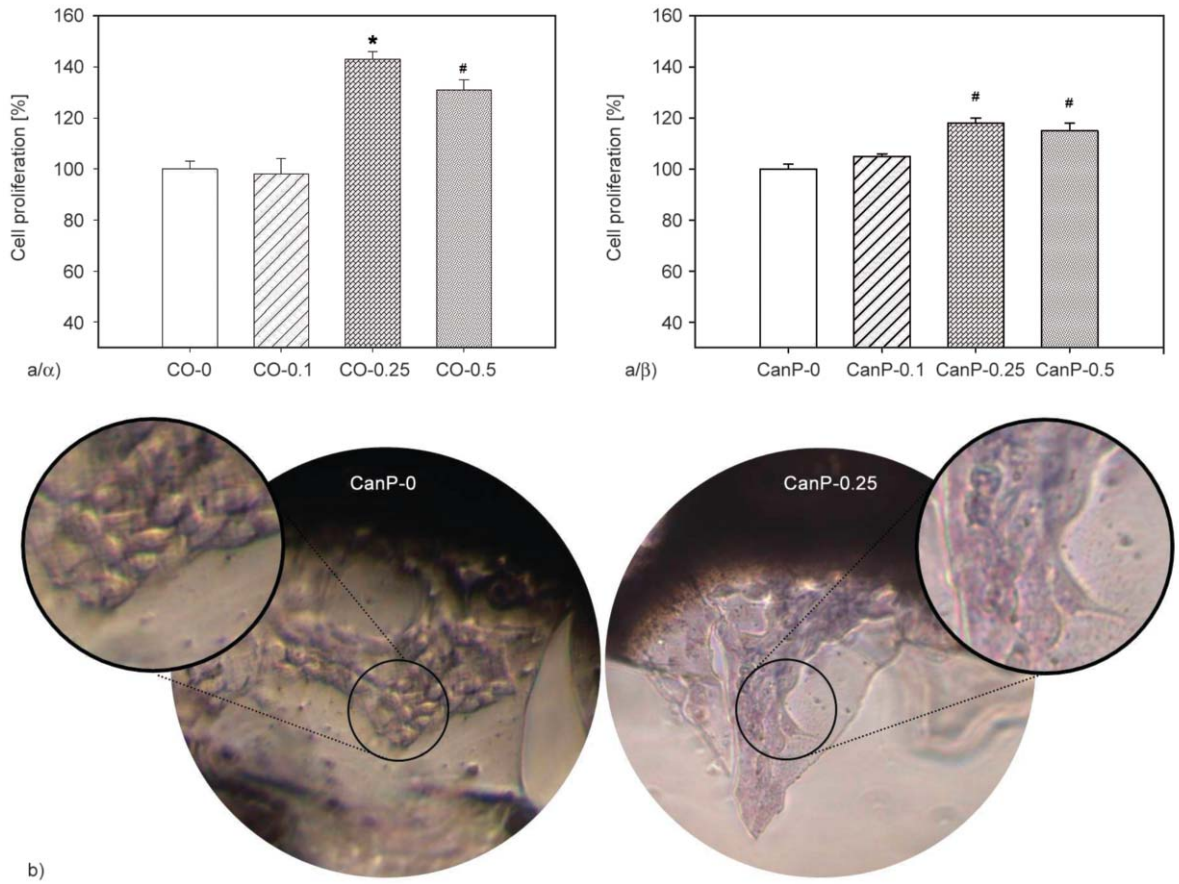

Figure 7. a) MC3T3-E1 cell proliferation using MTT assay on PUF based on CO (α) or PUF based on CanP (b). Values are expressed as % *versus* PU after 24 h of proliferation. *: $p < 0{,}01$; #: $p < 0{,}05$. b) Cell morphology of the MC3T3-E1 cells grown on the foams CanP-0 and CanP-0.25 for 24 h of culturing.

an improvement of the mechanical properties. When evaluating the proliferation of cells grown on different foams, it was observed that the presence of CN significantly increased the cell viability for samples containing 0.25 and 0.50 wt% of CN, while for the lowest concentration used no effect was observed. The results suggest that the incorporation of CN increases the biocompatibility of the PU foams, which place them as materials with potential biomedical applications.

Acknowledgements

This work was supported by the ANPCyT (PICT 2013-0643), UNAJ (project UNAJ Investiga 2014), and UNLP (PPID X028). We would like to thank Lidia Bruzza (Química R&F S.R.L.) and Alejandro de Gasperi (Mayerhofer Argentina S.A.) for supplying the reactants. MVG is a member of CIC-PBA and PJP is a member of CONICET.

References

[1] Nohra B., Candy L., Blanco J-F., Guerin C., Raoul Y., Mouloungui Z.: From petrochemical polyurethanes to biobased polyhydroxyurethanes. Macromolecules, **46**, 3771–3792 (2013). https://doi.org/10.1021/ma400197c

[2] Lligadas G., Ronda J. C., Galiá M., Cádiz V.: Plant oils as platform chemicals for polyurethane synthesis: Current state-of-the-art. Biomacromolecules, **11**, 2825–2835 (2010). https://doi.org/10.1021/bm100839x

[3] Das S., Pandey P., Mohanty S., Nayak S. K.: Insight on castor oil based polyurethane and nanocomposites: Recent trends and development. Polymer-Plastics Technology and Engineering, **56**, 1556–1585 (2017). https://doi.org/10.1080/03602559.2017.1280685

[4] Zlatanić A., Lava C., Zhang W., Petrović Z. S.: Effect of structure on properties of polyols and polyurethanes based on different vegetable oils. Journal of Applied Polymer Science, **42**, 809–819 (2004). https://doi.org/10.1002/polb.10737

[5] Kong X., Liu G., Curtis J. M.: Novel polyurethane produced from canola oil based poly(ether ester) polyols: Synthesis, characterization and properties. European Polymer Journal, **48**, 2097–2106 (2012). https://doi.org/10.1016/j.eurpolymj.2012.08.012

[6] Gama N. V., Ferreira A., Barros-Timmons A.: Polyurethane foams: Past, present, and future. Materials, **11**, 1841/1–1841/35 (2018) https://doi.org/10.3390/ma11101841

[7] Wang C., Zheng Y., Xie Y., Qiao K., Sun Y., Yue L.: Synthesis of bio-castor oil polyurethane flexible foams and the influence of biotic component on their performance. Journal of Polymer Research, **22**, 145/1–145/9 (2015). https://doi.org/10.1007/s10965-015-0782-7

[8] Narine S. S., Kong X., Bouzidi L., Sporns P.: Physical properties of polyurethanes produced from polyols from seed oils: II. Foams. Journal of the American Oil Chemists Society, **84**, 65–72 (2007). https://doi.org/10.1007/s11746-006-1008-2

[9] Stirna U., Lazdiņa B., Vilsone D., Lopez M. J., Vargas-García M. C., Suárez-Estrella F., Moreno J.: Structure and properties of the polyurethane and polyurethane foam synthesized from castor oil polyols. Journal of Cellular Plastics, **48**, 476–488 (2012). https://doi.org/10.1177/0021955X12445178

[10] Guo A., Javni I., Petrovic Z.: Rigid polyurethane foams based on soybean oil. Journal of Applied Polymer Science, **77**, 467–473 (2000). https://doi.org/10.1002/(SICI)1097-4628(20000711)77:2<467::AID-APP25>3.0.CO;2-F

[11] Hu Y. H., Gao Y., Wang D. N., Hu C. P., Zu S., Vanoverloop L., Randall D.: Rigid polyurethane foam prepared from a rape seed oil based polyol. Journal of Applied Polymer Science, **84**, 591–597 (2002). https://doi.org/10.1002/app.10311

[12] Gu R., Konar S., Sain M.: Preparation and characterization of sustainable polyurethane foams from soybean oils. Journal of the American Oil Chemists Society, **89**, 2103–2111 (2012). https://doi.org/10.1007/s11746-012-2109-8

[13] Zhang C., Kessler M. R.: Bio-based polyurethane foam made from compatible blends of vegetable-oil-based polyol and petroleum-based polyol. ACS Sustainable Chemistry and Engineering, **3**, 743–749 (2015) https://doi.org/10.1021/acssuschemeng.5b00049

[14] Kim M. W., Kwon S. H., Park H., Kim B. K.: Glass fiber and silica reinforced rigid polyurethane foams. Express Polymer Letters, **11**, 374–382 (2017). https://doi.org/10.3144/expresspolymlett.2017.36

[15] Adnan S., Tuan Ismail T. N. M., Mohd Noor N., Din N. S. M. N. M., Hanzah N. A., Shoot Kian Y., Abu Hassan H.: Development of flexible polyurethane nanostructured biocomposite foams derived from palm olein-based polyol. Advances in Materials Science and Engineering, **2016**, 4316424/1–4316424/12 (2016). https://doi.org/10.1155/2016/4316424

[16] Chen L., Rende D., Schadler L. S., Ozisik R.: Polymer nanocomposite foams. Journal of Material Chemistry A, **1**, 3837–3850 (2013) https://doi.org/10.1039/C2TA00086E

[17] Pauzi N. N. P. N., Majid R. A., Dzulkifli M. H., Yahya M. Y.: Development of rigid bio-based polyurethane foam reinforced with nanoclay. Composites Part B: Engineering, **67**, 521–526 (2014). https://doi.org/10.1016/j.compositesb.2014.08.004

[18] Panda S. S., Samal S. K., Mohanty S., Nayak S. K.: Preparation, characterization, and properties of castor oil-based flexible polyurethane/Cloisite 30B nanocomposites foam. Journal of Composite Materials, **52**, 531–542 (2018). https://doi.org/10.1177/0021998317710707

[19] Malewska E., Prociak A.: The effect of nanosilica filler on the foaming process and properties of flexible polyurethane foams obtained with rapeseed oil-based polyol. Polimery, **2015**, 472–479 (2015). https://doi.org/10.14314/polimery.2015.472

[20] Agrawal A., Kaur R., Walia R. S.: Development of vegetable oil-based conducting rigid PU foam. e-Polymers, **19**, 411–420 (2019). https://doi.org/10.1515/epoly-2019-0042

[21] Luo X., Yu Z., Cai Y., Wu Q., Zeng J.: Facile fabrication of environmentally-friendly hydroxyl-functionalized multiwalled carbon nanotubes/soy oil-based polyurethane nanocomposite bioplastics with enhanced mechanical, thermal, and electrical conductivity properties. Polymers, **11**, 763/1–763/12 (2019). https://doi.org/10.3390/polym11050763

[22] Habibi Y., Lucia L. A., Rojas O. J.: Cellulose nanocrystals: Chemistry, self-assembly, and applications. Chemical Reviews, **110**, 3479–3500 (2010). https://doi.org/10.1021/cr900339w

[23] Dufresne A.: Cellulose nanomaterials as green nanoreinforcements for polymer nanocomposites. Philosophical Transactions of the Royal Society A: Mathematical Physical and Engineering Sciences, **376**, 20170040/1–20170040/23 (2018). https://doi.org/10.1098/rsta.2017.0040

[24] Stepvani A. A., Evans D. A. C., Martin D. J., Annamalai P. K.: Hybrid polyether-palm oil polyester polyol based rigid polyurethane foam reinforced with cellulose nanocrystal. Industrial Crops and Products, **112**, 378–388 (2018). https://doi.org/10.1016/j.indcrop.2017.12.032

[25] Huang X., De Hoop C. F., Xie J., Wu Q., Boldor D., Qi J.: High bio-content polyurethane (PU) foam made from bio-polyol and cellulose nanocrystals (CNCs) via microwave liquefaction. Materials and Design, **138**, 11–20 (2018). https://doi.org/10.1016/j.matdes.2017.10.058

[26] Li Y., Ren H., Ragauskas A. J.: Rigid polyurethane foam reinforced with cellulose whiskers: Synthesis and characterization. Nano-Micro Letters, **2**, 89–94 (2010). https://doi.org/10.1007/BF03353624

[27] Li Y., Ren H., Ragauskas A. J.: Rigid polyurethane foam/cellulose whisker nanocomposites: Preparation, characterization, and properties. Journal of Nanoscience and Nanotechnology, **11**, 6904–6911 (2010). https://doi.org/10.1166/jnn.2011.3834

[28] Cordero A. I., Amalvy J. I., Fortunati E., Kenny J. M., Chiacchiarelli L. M.: The role of nanocrystalline cellulose on the microstructure of foamed castor-oil polyurethane nanocomposites. Carbohydrate Polymers, **134**, 110–118 (2015). https://doi.org/10.1016/j.carbpol.2015.07.077

[29] Zhou X., Sain M. M., Oksman K.: Semi-rigid biopolyurethane foams based on palm-oil polyol and reinforced with cellulose nanocrystals. Composites Part A: Applied Science and Manufacturing, **83**, 56–62 (2016). https://doi.org/10.1016/j.compositesa.2015.06.008

[30] Ugarte L., Santamaria-Echart A., Mastel S., Autore M., Hillendbrand R., Corcuera M. A., Eceiza A.: An alternative approach for the incorporation of cellulose nanocrystals in flexible polyurethane foams based on renewably sourced polyols. Industrial Crops and Products, **95**, 564–573 (2017). https://doi.org/10.1016/j.indcrop.2016.11.011

[31] Corsello F. A., Bolla P. A., Anbinder P. S., Serradell M. A., Amalvy J. I., Peruzzo P. J.: Morphology and properties of neutralized chitosan-cellulose nanocrystals biocomposite films. Carbohydrate Polymers, **156**, 452–459 (2017). https://doi.org/10.1016/j.carbpol.2016.09.031

[32] Reid M. S., Villalobos M., Cranston E. D.: Benchmarking cellulose nanocrystals: From the laboratory to industrial production. Langmuir, **337**, 1583–1598 (2017). https://doi.org/10.1021/acs.langmuir.6b03765

[33] Espinoza Pérez J. D., Haagenson D. M., Pryor S. W., Ulven C. A., Wiesenborn D. P.: Production and characterization of epoxidized canola oil. Transactions of the ASABE, **52**, 1289–1297 (2009). https://doi.org/10.13031/2013.27772

[34] Chen J., Soucek M. D., Simonsick W. J., Celikay R. W.: Epoxidation of partially norbornylized linseed oil. Macromolecular Chemistry and Physics, **203**, 2042–2057 (2002). https://doi.org/10.1002/1521-3935(200210)203:14<2042::AID-MACP2042>3.0.CO;2-0

[35] Vlček T., Petrović Z. S.: Optimization of the chemoenzymatic epoxidation of soybean oil. Journal of the American Oil Chemists' Society, **83**, 247–252 (2006). https://doi.org/10.1007/s11746-006-1200-4

[36] Mosiewicki M. A., Rojek P., Michałowski S., Aranguren M. I., Prociak A.: Rapeseed oil-based polyurethane foams modified with glycerol and cellulose micro/nanocrystals. Journal of Applied Polymer Science, **132**, 41602/1–41602/8 (2015). https://doi.org/10.1002/app.41602

[37] Gómez-Ordóñez E., Rupérez P.: FTIR-ATR spectroscopy as a tool for polysaccharide identification in edible brown and red seaweeds. Food Hydrocolloids, **25**, 1514–1520 (2011). https://doi.org/10.1016/j.foodhyd.2011.02.009

[38] Mandal A., Chakrabarty D.: Isolation of nanocellulose from waste sugarcane bagasse (SCB) and its characterization. Carbohydrate Polymers, **86**, 1291–1299 (2011). https://doi.org/10.1016/j.carbpol.2011.06.030

[39] Parada Hernandez N. L., Bonon A. J., Bahú J. O., Barbosa M. I. R., Maciel M. R. W, Maciel Filho R.: Epoxy monomers obtained from castor oil using a toxicity-free catalytic system. Journal of Molecular Catalysis A: Chemical, **426**, 550–556 (2017). https://doi.org/10.1016/j.molcata.2016.08.005

[40] Petrović Z. S., Zavargo Z., Flynn J. H., Macknight W. J.: Thermal degradation of segmented polyurethanes. Journal of Applied Polymer Science, **51**, 1087–1095 (1994). https://doi.org/10.1002/app.1994.070510615

[41] Aoyagi Y., Yamashita K., Doi Y.: Thermal degradation of poly[(R)-3-hydroxybutyrate], poly[ε-caprolactone], and poly[(S)-lactide]. Polymer Degradation and Stability, **76**, 53–59 (2002). https://doi.org/10.1016/S0141-3910(01)00265-8

[42] Chrissafis K., Paraskevopoulos K. M., Bikiaris D. N.: Thermal degradation kinetics of the biodegradable aliphatic polyester, poly(propylene succinate). Polymer Degradation and Stability, **91**, 60–68 (2006). https://doi.org/10.1016/j.polymdegradstab.2005.04.028

[43] Kong X., Narine S. S.: Physical properties of polyurethane plastic sheets produced from polyols from canola oil. Biomacromolecules, **8**, 2203–2209 (2007). https://doi.org/10.1021/bm070016i

[44] Eychenne V., Mouloungui Z., Gaset A.: Thermal behavior of neopentylpolyol esters: Comparison between determination by TGA-DTA and flash point. Thermochimica Acta, **320**, 201–208 (1998). https://doi.org/10.1016/S0040-6031(98)00466-3

[45] Lin B., Yang L., Dai H., Hou Q., Zhang L.: Thermal analysis of soybean oil based polyols. Journal of Thermal Analysis and Calorimetry, **95**, 977–983 (2009). https://doi.org/10.1007/s10973-007-8929-3

[46] dos Santos Politi J. R., de Matos P. R. R., Araújo Sales M. J.: Comparative study of the oxidative and thermal stability of vegetable oils to be used as lubricant bases. Journal of Thermal Analysis and Calorimetry, **111**, 1437–1442 (2013). https://doi.org/10.1007/s10973-012-2529-6

[47] Cao X., Habibi Y., Lucia L. A.: One-pot polymerization, surface grafting, and processing of waterborne polyurethane-cellulose nanocrystal nanocomposites. Journal of Material Chemistry, **19**, 7137–7145 (2009). https://doi.org/10.1039/B910517D

[48] Celebi H., Kurt A.: Effects of processing on the properties of chitosan/cellulose nanocrystal films. Carbohydrate Polymers, **133**, 284–293 (2015). https://doi.org/10.1016/j.carbpol.2015.07.007

[49] Yeganeh H., Hojati-Talemi P.: Preparation and properties of novel biodegradable polyurethane networks based on castor oil and poly(ethylene glycol). Polymer Degradation and Stability, **92**, 480–489 (2007). https://doi.org/10.1016/j.polymdegradstab.2006.10.011

[50] Ramakrishna S., Huang Z-M.: Biocomposites. Comprehensive Structural Integrity, **9**, 215–296 (2003). https://doi.org/10.1016/B978-0-12-803581-8.00965-6

[51] Kong X., Liu G., Qi H., Curtis J. M.: Preparation and characterization of high-solid polyurethane coating systems based on vegetable oil derived polyols. Progress in Organic Coatings, **76**, 1151–1160 (2013). https://doi.org/10.1016/j.porgcoat.2013.03.019

[52] Shahrousvand E., Shahrousvand M., Ghollasi M., Seyedjafari E., Jouibari I. S., Babaei A., Salimi A.: Preparation and evaluation of polyurethane/cellulose nanowhisker bimodal foam nanocomposites for osteogenic differentiation of hMSCs. Carbohydrate Polymers, **171**, 281–291 (2017). https://doi.org/10.1016/j.carbpol.2017.05.027